

# Thermal Decomposition of 1,3,5,5-Tetranitrohexahydro-Pyrimidine: A New Type of Autocatalysis that Persists at High Temperatures

Valery P. Sinditskii,<sup>\*[a]</sup> Anastasia D. Smirnova,<sup>[a]</sup> Tuan Q. Vu,<sup>[a]</sup> Sergey A. Filatov,<sup>[a]</sup> Valery V. Serushkin,<sup>[a]</sup> and Gennady F. Rudakov<sup>[a]</sup>

**Abstract:** The thermal stability of 1,3,5,5-tetranitrohexahydro-pyrimidine (TNDA) in liquid phase under isothermal conditions was studied. It was established that the TNDA decomposition ( $k_{\text{liq}} = 3.1 \cdot 10^{21} \cdot \exp(-26865/T)$ ,  $E_a = 223.4 \text{ kJ mol}^{-1}$ ) is accompanied by strong autocatalysis ( $k_{\text{cat}} = 9.8 \cdot 10^{14} \cdot \exp(-18056/T)$ ,  $E_a = 150.2 \text{ kJ mol}^{-1}$ ). The mechanism of autocatalysis was proposed. The essence of autocatalysis is the oxidation of TNDA by decomposition products, followed by the destruction of the molecule. An

unusual feature of this autocatalysis is that, in contrast to autocatalysis of nitroesters, the process does not disappear at high temperatures, but rather determines the kinetics of heat release in the combustion wave. The surface temperature and combustion mechanism of TNDA were established through thermocouple studies. It was shown that the autocatalysis reaction at the surface temperature controls the burning rate.

**Keywords:** Decomposition kinetics · 1,3,5,5-Tetranitrohexahydropyrimidine · Combustion · Vapor · Pressure

## 1 Introduction

The performance of an explosive depends on the enthalpy of formation of the substance and its elemental composition. In most cases, the molecule of energetic material contains an excess of atoms capable of oxidation (C and H). Improving the oxygen balance is achieved by increasing the number of nitro groups in the molecule. One of the tested ways is the replacement of the nitramine group with a gem-dinitromethyl fragment. A well-known example of this method is 1,3,5,5-tetranitrohexahydro-pyrimidine (TNDA or DNNC) (Figure 1). TNDA is an analogue of the known explosive 1,3,5-trinitro-1,3,5-triazine (RDX). TNDA was first synthesized in the early 1980s [1] and was patented as a component for explosive compositions and rocket propellants [2].

TNDA has high density ( $1.82 \text{ g cm}^{-3}$  at  $23^\circ\text{C}$ ), positive heat of formation ( $+53.1 \text{ kJ mol}^{-1}$ ), which provides high detonation velocity and detonation pressure:  $8.73 \text{ km s}^{-1}$  and  $34 \text{ GPa}$ , respectively [1]. In subsequent studies, an X-ray diffraction analysis of TNDA was performed, according to which the substance crystallizes in rhombic symmetry with

a density of  $1.80 \text{ g cm}^{-3}$  [3]. TNDA enthalpy of formation, measured later, is also lower:  $-7.9 \text{ kJ mol}^{-1}$  [4] and even  $-0.21 \text{ kJ mol}^{-1}$  [5]. Nevertheless, it is obvious that TNDA is superior to RDX in energetic performance, and lower sensitivity to mechanical stimuli makes this substance quite attractive for researchers in many countries [6–10]. According to [8], TNDA gave  $H_{50\%} = 85 \text{ cm}$  in an impact sensitivity test, which indicates that it is less sensitive than RDX ( $H_{50\%} = 28\text{--}30 \text{ cm}$ ). TNDA is also insensitive to friction and electrostatic discharge [1]. High oxygen content in molecule allows considering TNDA as energetic filler reducing smoke formation in solid propellants [10].

Various methods of TNDA synthesis based on nitration of dialkyl derivates of gem-dinitropyrimidine produced by Mannich cyclization from dinitropropanediol have been proposed [6, 11, 12]. In study [13] effective scheme of TNDA synthesis from nitromethane with intermediate formation of 3-tert-butyl-5,5-dinitrotetrahydro-1,3-oxazine succeeded by 1,3-di-tert-butyl-5,5-dinitrohexahydro-pyrimidine was developed. The total yield of TNDA by this method is 46%, that is rather more than 15% and 35% yield of previously proposed methods [1, 6, 11, 12].

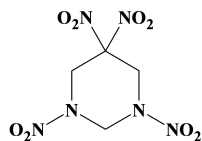


Figure 1. Structural formula of TNDA.

[a] V. P. Sinditskii, A. D. Smirnova, T. Q. Vu, S. A. Filatov, V. V. Serushkin, G. F. Rudakov  
Chemical Engineering Department  
Mendeleev University of Chemical Technology,  
9 Miusskaya Sq., Moscow, Russia  
(+7)495-4966027  
*\*e-mail: vps@rctu.ru*

According to DSC data, the melting point of TNDA lies in the temperature range 151–154 °C [1] (153.3–153.8 °C [14]), heat of melting 22.34 kJ mol<sup>-1</sup> [14]. Decomposition temperatures of TNDA (219 °C at 10 °C min<sup>-1</sup> [13]) and RDX are comparable with each other, but quite significant temperature range exists between melting point and decomposition temperature of TNDA in contrast to RDX. The heat of TNDA decomposition is 795 kJ mol<sup>-1</sup> or 2989 kJ kg<sup>-1</sup> [15]. According to the TGA, the mass loss in the temperature interval between melting and decomposition is 57% [8] or 81% [15], another 18% of the mass loss [8] is not accompanied by heat release.

Study of TNDA thermolysis using fast scanning Fourier infrared spectroscopy showed that NO<sub>2</sub> is the dominant initial pyrolysis product [16]. In addition, the formation of HONO is observed in the early stages. The authors associated NO and CO<sub>2</sub> formation with nitro-nitrite isomerization and decomposition of the C(NO<sub>2</sub>)<sub>2</sub> group. N<sub>2</sub>O is formed in gaseous products of TNDA, but in contrast to RDX, CH<sub>2</sub>O is absent, which may indicate its rapid consumption in the melt. In a subsequent work [17], when simulating TNDA combustion by rapid heating of a sample and “quenching” of decomposition products in cold Ar, they showed that the initial products are NO<sub>2</sub> and CO<sub>2</sub>, and after combustion (most likely, after a thermal explosion), the content of NO<sub>2</sub>, CH<sub>2</sub>O, NO and CO<sub>2</sub> increases sharply. N<sub>2</sub>O, CO, HONO and HCN also appear in lesser concentrations.

The data of [15], in which the kinetic deuterium isotope effect (KDIE) was discovered, turned out to be in contrast with these results. The authors concluded that the cleavage of the C–H bond determines the endothermic initiation and subsequent exothermic propagating energy release rates.

The initial step of thermal decomposition of nitramines is the breaking of N–NO<sub>2</sub> bond. For TNDA in which both N–NO<sub>2</sub> and C–NO<sub>2</sub> exist, the NO<sub>2</sub> fission reaction from C–NO<sub>2</sub> group may compete with that from N–NO<sub>2</sub> group. The authors in work [18] studied decomposition pathways of TNDA by using the B3LYP/6-31+G (d,p) method and found that initial steps of thermal decomposition of TNDA to be barrierless N–NO<sub>2</sub> and C–NO<sub>2</sub> fission with reaction energies of 156.5 and 145.9 kJ mol<sup>-1</sup>, respectively. Therefore, despite close energies, preference should be given to breaking the C–NO<sub>2</sub> bond. In contrast, a manometric study led to the conclusion that a combination of secondary nitramino groups with oxo, gem-dinitro and tetrazolyl group in a six-membered heterocycle does not change the limiting stage of thermolysis, viz. N–N homolysis, but can increase thermolysis rate by 2–7 orders of magnitude [19].

The kinetic parameters of TNDA decomposition were determined under nonisothermal conditions by the TGA method [8] ( $E_a=153.1\text{ kJ mol}^{-1}$ , logA=14.28) and using isothermal DSC [15]. In the latter case, the authors indicate that the decomposition process is autocatalytic in nature:

the initial endothermic process has an activation energy of  $E_a=169.9\text{ kJ mol}^{-1}$ , and for the acceleration stage  $E_a=104.2\text{ kJ mol}^{-1}$ . However, only one set of constants for the autocatalytic stage is given in the work, which is an order of magnitude higher than the rate constants obtained under nonisothermal conditions using TGA [8]. Manometric study of TNDA decomposition also indicates the autocatalytic nature of the process [19]. However, the kinetic parameters of only the “limiting” reaction ( $E_a=159.0\text{ kJ mol}^{-1}$ , logA=14.71) are presented, which are close to the TGA data, given in the work [8].

Thus, despite the long history of TNDA studies, there is no unambiguous decomposition mechanism, the nature of autocatalysis is not clear, and the kinetic parameters of decomposition raise questions. The aim of this study was to study the thermal decomposition of TNDA over a wide temperature range, both in non-isothermal and isothermal conditions, which could give a clearer picture of the process.

## 2 Experimental Section

**Preparation.** 1,3-Di-tert-butyl-5,5-dinitrohexahydro-pyrimidine was prepared by boiling 3-(tert-butyl)-5,5-dinitro-1,3-oxazinane with tert-butylamine in ethanol, according to published method [13].

**1,3,5,5-Tetranitrohexahydropyrimidine (TNDA):** To concentrated sulfuric acid (35 mL, 94%) at 0–3 °C was added the 1,3-di-tert-butyl-5,5-dinitrohexahydropyrimidine (2.88 g, 10 mmol) over a 30 min period. A mixture of nitric (6 ml, 98%) and sulfuric acids (11 ml, 94%) was added and the resulting mass was stirred for 1 h at 0 °C and for 2 h at room temperature and then poured onto ice (200 g). The product was extracted with dichloromethane, and the organic phase was then washed with cold water and dried on sodium sulphate. The solvent was evaporated and solid was purified by column chromatography on silica gel using trichloromethane as eluent. Yield 2.15 g (81%), colorless crystals, mp. 153–154 °C. IR spectrum,  $\nu$ , cm<sup>-1</sup>: 3088, 3066, 3036 (CH); 1577, 1316, 1296 (NO<sub>2</sub>). <sup>1</sup>H NMR spectrum,  $\delta$ , ppm: 5.34 (4H, s, N–CH<sub>2</sub>–C); 6.11 (2H, s, C–CH<sub>2</sub>–C). <sup>13</sup>C NMR spectrum,  $\delta$ , ppm: 48.49; 58.98; 106.72. Mass spectrum (LCMS, ESI),  $m/z$  (I<sub>rel</sub>, %): 577 [2M+HCOO]<sup>-</sup> (100), 311 [M+HCOO]<sup>-</sup> (15). Found, %: C 18.07; H 2.15; N 31.81. C<sub>4</sub>H<sub>6</sub>N<sub>6</sub>O<sub>8</sub>. Calculated, %: C 18.05; H 2.27; N 31.58.

**Decomposition Study.** The thermal stability of TNDA was investigated under non-isothermal conditions using differential scanning calorimetry (DSC) as well as under isothermal conditions by means of the manometric method.

DSC studies were performed with DSC 822e Mettler Toledo in the temperature range of 25–300 °C at different heating rates. The samples weighing between 1 and 2 mg were analyzed in closed aluminum pans with pierced lids. Kinetic parameters of thermal decomposition were calcu-

lated using Kissinger's equation [20], assuming that the reaction is first order:

$$\ln \frac{\varphi}{T_{\max}^2} = \ln \frac{AR}{E} - \frac{E}{RT_{\max}},$$

where  $\varphi$  is heating rate (K/s),  $E$  is activation energy,  $A$  is pre-exponential factor,  $T_{\max}$  is maximal temperature of exotherm. The results are presented in Table 1.

Experiments on isothermal decomposition of TNDA were carried out in thin-walled glass manometers of the compensation type (the glass Bourdon gauge). A sample (10–15 mg) was loaded into a glass manometer of 10–15 cm<sup>3</sup> volume. The device was evacuated to 13.3 Pa, sealed, and immersed in a thermostat with Wood's metal alloy. The temperature in the thermostat was maintained with an accuracy of  $\pm 0.5^\circ\text{C}$ . The pressure of gases evolving in the course of decomposition (the accuracy of pressure measurements was  $\pm 13.3$  Pa) was monitored and then converted to the gas volume at normal conditions ( $20^\circ\text{C}$ , 0.1 MPa). Because of the autocatalytic nature of the decomposition process, the rate constants were calculated using the model of first-order reaction with self-acceleration  $V =$

$V_\infty \cdot k_{liq} \cdot (\exp((k_{liq} + k_{cat}) \cdot t) - 1) / (k_{cat} + k_{liq} \cdot \exp((k_{liq} + k_{cat}) \cdot t))$ , where  $V_\infty$  is maximum volume of gas evolved per gram of compound,  $k_{liq}$  is the rate constant of the non-catalytic stage in the liquid state,  $k_{cat}$  is the pseudo first-order rate constant of the catalytic stage, and  $t$  is time (Table 2).

**Combustion Study.** Burning rates ( $r_b$ ) of TNDA were measured in a window constant-pressure bomb of 1.5-liter volume in the 0.1–10 MPa pressure interval. The bomb was pressurized with nitrogen. Samples to test were prepared as pressed cylinders of pure compounds with 4–5 mm height confined in transparent acrylic tubes of 4 mm i.d. and 6 mm o.d. The combustion process was recorded with a high-speed video camera. The burning rate was determined by measuring the position of the flame front over time. The density of the pressed pellets ( $\rho_{press}$ ), percent of theoretical maximum density (%TMD), oxidizer/fuel ratio ( $\alpha$ ), enthalpy of formation ( $\Delta H_f^\circ$ ), calculated adiabatic flame temperature ( $T_{ad}$ ), burning rate at 10 MPa, and burning rate law ( $r_b = bP^n$ ) parameters for the studied compound in comparison with RDX are presented in Table 3.

The adiabatic flame temperature was calculated with the "REAL" computer code for simulation of the chemical equilibrium at high temperature and pressure [21].

Temperature profiles in the combustion wave were measured using fine tungsten-rhenium thermocouples. The thermocouples were welded from 80%W+20%Re and 95%W+5%Re wires, 25  $\mu\text{m}$  thick, followed by rolling in bands 5–7  $\mu\text{m}$  thick. The thermocouple was embedded into the center of the sample. The method of preparation of the samples used in the temperature profile measurements was previously described in detail in Ref. [22]. The thermocouple signal was recorded with a Picotech 12-bit digital oscilloscope.

Based on one-dimensional conductive heat transfer analysis, the thermal diffusivity ( $\chi$ ) of molten compounds may be evaluated from the temperature distribution in the condensed phase. A plot of  $\ln(T-T_0)/(T_s-T_0)$  versus distance yields a straight line with the slope equal to  $r_b/\chi$ . The results of the investigation are presented in Table 4.

**Analysis.** IR spectra were recorded on a Thermo Nicolet 360 FTIR spectrometer in KBr pellets. <sup>1</sup>H and <sup>13</sup>C NMR spectra were acquired on a Varian Mercury Plus instrument (400 and 100 MHz, respectively) for solutions in DMSO-*d*<sub>6</sub> at 50 °C. Residual solvent signals were used as internal standard for <sup>1</sup>H and <sup>13</sup>C NMR spectra (2.50 and 39.5 ppm, respectively). LC/MS analysis was performed on

**Table 1.** Results of DSC study of TNDA.

Heating rate, °C min <sup>-1</sup>	T <sub>max</sub> , °C	k · 10 <sup>3</sup> , s <sup>-1</sup>
2	199	2.7
4	204	5.3
4	202	5.4
8	213	10.3
16	224	19.7
16	217	20.3

**Table 2.** Results of isothermal decomposition study of TNDA.

Temperature, °C	Rate constant ( $\cdot 10^5$ s <sup>-1</sup> )	
	k <sub>liq</sub>	k <sub>cat</sub>
160	0.31	74.8
165	0.80	134.0
165	0.66	120.0
170	1.48	172.3
170	1.54	198.8
175	3.10	321.2
180	4.59	478.2

**Table 3.** Combustion characteristics of TNDA and RDX.

Compound	$\alpha$	$\Delta H_f^\circ$ , kJ kg <sup>-1</sup>	$\rho_{press}$ (%TMD) g cm <sup>-3</sup>	T <sub>ad</sub> at 10 MPa, K	$r_b = bP^n$ (mm s <sup>-1</sup> ) in interval 0.1–10 MPa	$r_b$ at 10 MPa, mm s <sup>-1</sup>
TNDA	0.727	−25.2	1.70 (94)	3440	2.11	0.86
RDX	0.667	301.3	1.75 (97)	3310	2.66	0.83

**Table 4.** The thermal diffusivity,  $\chi$ , and characteristic temperatures in the combustion wave of TNDA.

Compound	$\chi \cdot 10^3$ , $\text{cm}^2 \cdot \text{s}^{-1}$	Pressure, MPa	$T_s$ , C <sup>[a]</sup>	$T_1$ , C <sup>[a]</sup>	$T_f$ , C <sup>[a]</sup>
TNDA	1.1 ± 0.2	0.3	298 ± 8	820 ± 20	–
		0.4	312 ± 8	800	2255
		0.5	350 ± 9		2190 ± 75

<sup>[a]</sup> – Confidence intervals are given for three and more parallel runs.

a Thermo Scientific Ultimate3000/LTQ Fleet LT instrument under gradient elution conditions, using electrospray ionization (ESI) at atmospheric pressure with simultaneous recording of positively and negatively charged ions. The following chromatography conditions were used: RSLC 120 C18 column ( $2.1 \times 150$  mm), mobile phase –  $\text{H}_2\text{O}$ –MeCN with 0.1% (vol.) HCOOH and 0.3% (vol.)  $\text{NH}_4\text{OH}$  (25%), elution flow rate –  $0.3 \text{ ml} \cdot \text{min}^{-1}$ , temperature column –  $40^\circ\text{C}$ . Elemental analysis was performed on a PerkinElmer 2400 Series II CHNAnalyzer. Melting points were determined on a Boetius hot stage. The obtained compounds were purified by column chromatography on Durasil H 40–63  $\mu\text{m}$  silica gel.

### 3 Results and Discussion

#### 3.1 The Thermal Stability

The thermal stability of TNDA was initially evaluated using DSC in non-isothermal conditions. Using the Kissinger method [20] according to the maximum heat release at different heating rates under the assumption that the reaction proceeds in the first order, the rate constants TNDA were calculated, which are described by the equation  $k(\text{s}^{-1}) = 1.2 \cdot 10^{14} \cdot \exp(-17950/T)$  with an activation energy of  $149.4 \text{ kJ mol}^{-1}$ . The kinetic data turned out to be close to the data obtained previously using TGA [8].

Decomposition under isothermal conditions in a Bourdon manometer proceeds with acceleration, with the release of a large amount of gases  $\sim 620 \text{ cm}^3 \text{ g}^{-1}$  (7.4 mol/mol) (Figure 2). On cooling to room temperature,  $\sim 130 \text{ cm}^3 \text{ g}^{-1}$  gases (1.6 mol/mol) are condensed, while the yellow solidified melt is at the bottom of the vessel, brown gases are practically absent. In the IR spectrum of condensed decomposition products (sample in KBr), absorption bands of the O–H bond, carbonyl group ( $1751, 1686 \text{ cm}^{-1}$ ),  $\text{CH}_2$ -group ( $1432, 760 \text{ cm}^{-1}$ ) and nitrate anion ( $1385 \text{ cm}^{-1}$ ) are observed.

Gas evolution curves only up to degree of decomposition of 0.15 ( $\sim 90 \text{ cm}^3 \text{ g}^{-1}$ ) are described by a equation of first-order with autocatalysis, then the acceleration becomes even greater (Figure 2).

The rate constants of the non-catalytic stage of decomposition of the substance ( $k_{liq} = 3.1 \cdot 10^{21} \cdot \exp(-26865/T)$ )

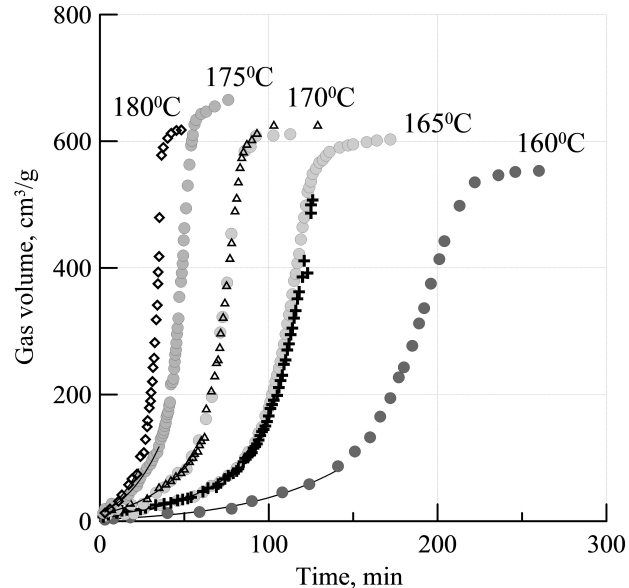


**Figure 2.** Gas release curves for TNDA decomposition at different temperatures. Points are an experiment, lines are a model description.

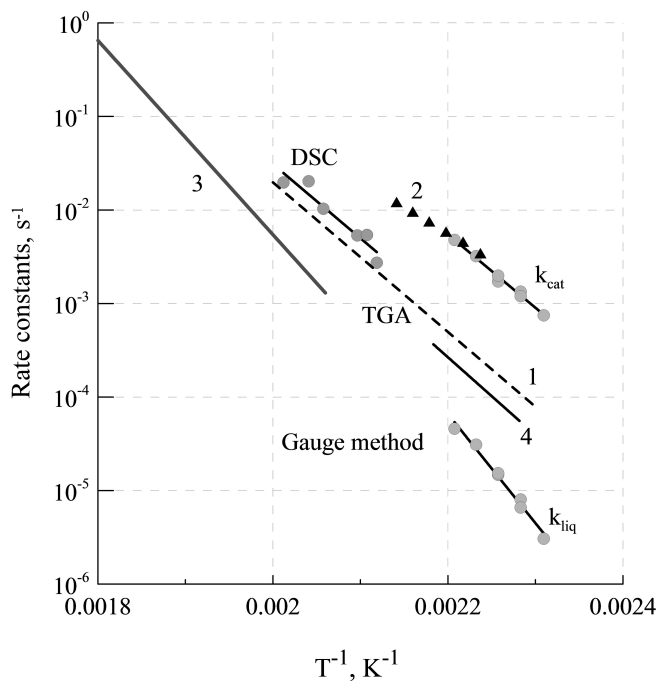


**Figure 3.** Comparison of the kinetics of TNDA decomposition in nonisothermal (DSC, 1 (TGA) [8]) and isothermal ( $k_{liq}$ ,  $k_{cat}$ , 2 [15], 4 [19]) conditions with the kinetics of RDX decomposition in the liquid phase (3 [23]).

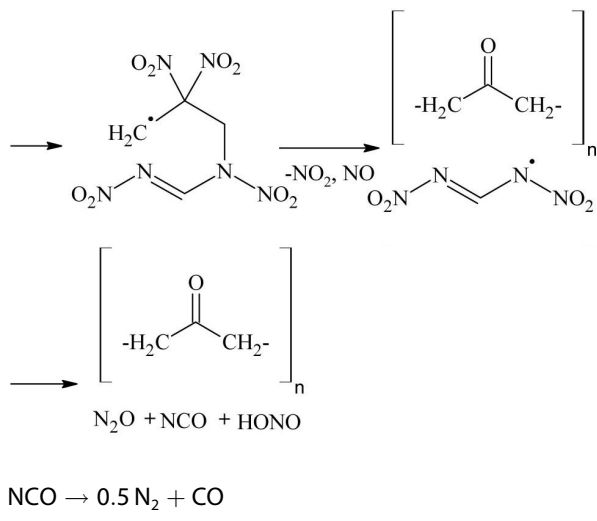
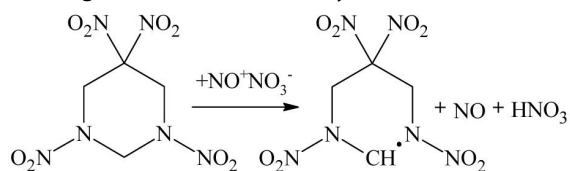
with an activation energy of  $223.4 \text{ kJ mol}^{-1}$  (Figure 3) characterize the initial decomposition in the liquid phase. The obtained constants are comparable to the RDX decomposition constants extrapolated from higher temperatures

[23], which indicates the similarity of the initial decomposition stage. The rate constants of autocatalysis ( $k_{cat} = 9.8 \cdot 10^{14} \cdot \exp(-18060/T)$ ) practically coincide with the data of isothermal decomposition under DSC conditions [15], but the activation energy turned out to be somewhat higher ( $150.2 \text{ kJ mol}^{-1}$ ). At the same time, the kinetics obtained under non-isothermal conditions (DSC and TGA) do not adequately describe the decomposition process. As can be seen from Figure 3, the rate constants of the “limiting” stage determined in [19] using a similar gauge method also do not agree with the initial step of decomposition of TNDA ( $k_{liq}$ ).

The decomposition mechanism proposed in [17] assumed the initial splitting of the C–NO<sub>2</sub> bond followed by the interaction of NO<sub>2</sub> with the radical center. However, this mechanism is inconsistent with the conclusion of [15] that C–H bond rupture regulates the propagation of the decomposition process. Monomolecular cleavage of HONO occurs during the decomposition of both nitroaliphatic compounds and nitramines [24]. This decay channel is consistent with the observed KDIЕ, but cannot explain the appearance of strong autocatalysis. The autocatalysis, which occurs in nitroesters, where the key stage is the formation of hydrolytically unstable nitrite from nitrate under the influence of decomposition products [25] also cannot be realized in this case.

One of the possible mechanisms of nitration in the liquid phase involves a single-electron-transfer step from the substrate to the nitronium or nitrosonium ion as the initial step with the intermediate formation of a radical cation [26]. It is quite obvious that nitrosonium ions can also form in the TNDA melt at high temperatures from nitrogen oxides that are split off at the first stage: NO<sub>2</sub>+NO<sub>2</sub>→NO<sup>+</sup>NO<sub>3</sub><sup>-</sup>.

The single-electron-transfer from the initial TNDA molecule to the nitrosonium ion will lead to the formation of a radical cation, which, by ejecting a proton, turns into a radical. The carbon atom with the most mobile protons is located between two nitramine groups [15]. Further destruction of the radical at high temperature leads to the formation of a polymer (for example, polyketones [27]) from the dinitroalkyl moiety and N<sub>2</sub>O, NCO and HONO from the nitramine fragment. The interaction of nitric and nitrous acid regenerates the autocatalyst:



This mechanism is consistent with the initial process of NO<sub>2</sub> elimination and explains the participation of the hydrogen atom in the rate-determining stage. The amount of gaseous products (6.5 mol, 79% of the mass of the substance, 1 molecule of condensing water) is close to the manometry data and is consistent with the mass loss in the TGA experiment [15]. The absence of NO<sub>2</sub> in gauge experiments can be associated with the reaction NO<sub>2</sub>+NCO→N<sub>2</sub>O+CO<sub>2</sub>. The composition of the polymer decomposition product is confirmed by IR spectroscopy data; strong absorption of the nitrate anion in the IR spectrum of indicates the presence of nitric acid.

In the case of nitroesters, autocatalysis plays an important role at the storage and processing temperatures of compositions based on them, but in the melt in the combustion wave at high temperatures, its contribution due to the low activation energy is practically insignificant [28]. To estimate the contribution of TNDA autocatalysis at high temperatures, it is necessary to know its burning rates and surface temperature.

TNDA combustion was investigated in the range of 2–25 MPa by French researchers [17]. It turned out that TNDA burning behavior is similar to those of the RDX. Based on Fourier spectroscopic data on the decomposition of these substances, the authors of [17] concluded that the closeness of the combustion rates is due to the fact that in both cases the combustion rate is controlled by the reactions of NO<sub>2</sub> and CH<sub>2</sub>O in the first flame. Note that the leading role of the condensed phase in the combustion of RDX was proved in the work [29].

In this work, TNDA combustion was studied in the pressure range 0.1–10 MPa in a nitrogen atmosphere. TNDA begins to burn steadily from 0.3 MPa, its burning rate ( $r_b = 0.75 \cdot P^{0.86}$ ) almost completely coincides with the previously obtained data [17] and is slightly lower than the burning rate of the nitramine RDX [19] (Figure 4).

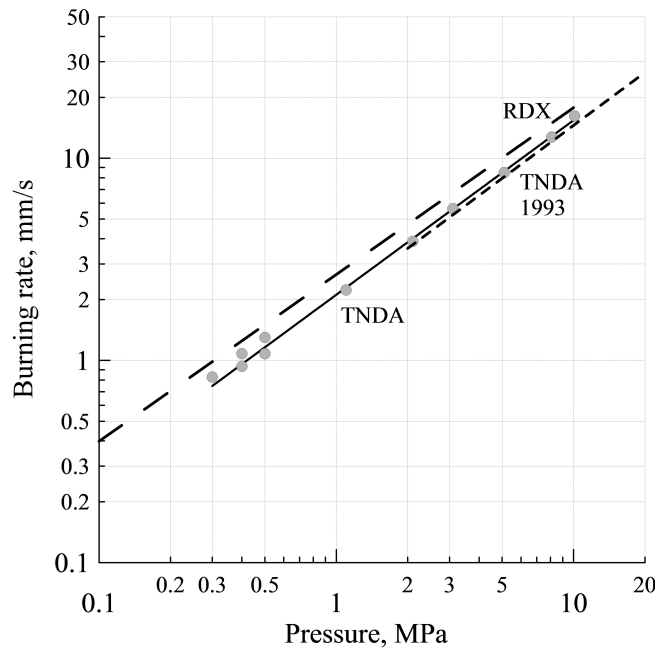


Figure 4. Comparison of TNDA burning rates with previously obtained results [17] and RDX.

The authors of [17] attempted to extract the TNDA decomposition kinetics from the combustion wave. They compensated for the lack of data on the surface temperature by suggesting that it should be 100–150 degrees above the decomposition temperature. The kinetic data from their experiments are 8 orders of magnitude higher than the rate constants obtained using TGA [8].

In order to obtain kinetic data, it is necessary not only to know the dependence of the surface temperature on pressure, but also to establish the combustion mechanism of the substance [30]. In this work, the temperature distribution in the TNDA combustion wave was studied at pressures of 0.3, 0.4, and 0.5 MPa, using thin tungsten-rhenium thermocouples. Typical TNDA temperature profiles are shown in Figure 5.

Thermocouple studies have shown that the gas phase has a two-flame structure. At a pressure of 0.3 MPa, only the first flame is observed, the temperature of which does not exceed 800 °C. The second high-temperature flame ignites already at 0.4 MPa, however, there is a 0.1–0.15 mm section between the surface and the high-temperature flame with a low temperature gradient even at 0.5 MPa (Figure 5). The heat release in the first flame is 1255–1340 J g<sup>-1</sup>, which is much less than the heat release under DSC conditions [15]. The maximum measured flame temperature of 2200 °C is also below the calculated adiabatic temperature (2845 °C), which is due to the loss of the thermocouple to radiation at high temperatures and incomplete response at low pressures.

Thermocouple studies provide surface temperature ( $T_s$ ) measurements. As can be seen from Figure 6, the surface

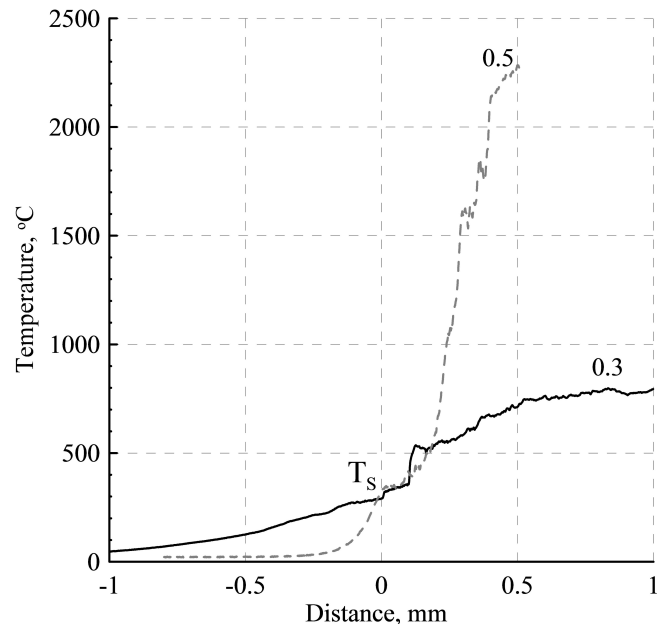


Figure 5. Typical TNDA temperature profiles. The numbers are pressure in MPa.

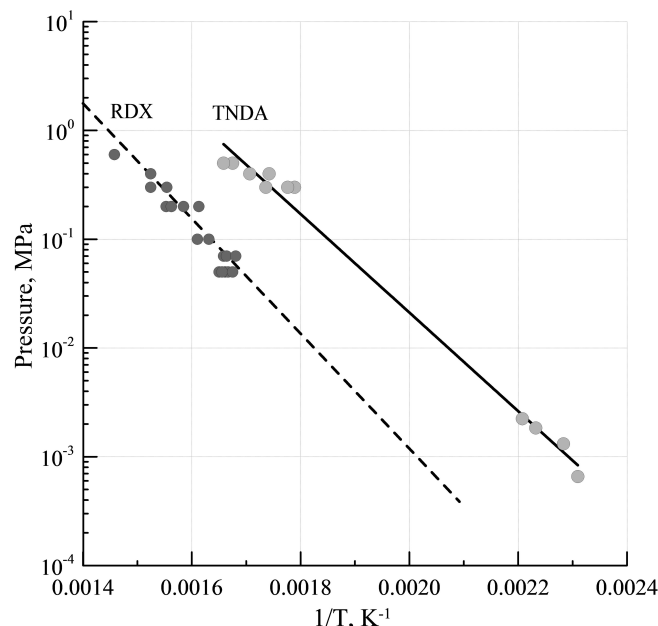


Figure 6. Comparison of surface temperatures TNDA and RDX.

temperature of TNDA is significantly lower than the surface temperature of RDX [30]. If we combine the thermocouple data with the initial pressure in the Bourdon manometer, we can obtain the dependence of the TNDA vapor pressure on temperature in a wide temperature range:  $\ln P = -10440/T + 17.02$ . According to this dependence, the heat of vaporization TNDA is 86.6 kJ mol<sup>-1</sup>, and the boiling point is 267 °C (101.3 kJ mol<sup>-1</sup> and 338 °C for RDX). Thus, the re-

placement of the nitramine fragment by the dinitroalkyl grouping leads to an increase in the volatility of the substance.

The obtained heat of vaporization together with the heat of fusion [14] allows choice of the correct value of the enthalpy of formation. The enthalpy of formation of gaseous TNDA ( $102.1 \text{ kJ mol}^{-1}$ ) was calculated in [31], using the density functional theory with B3LYP parametrization. Based on these data, the enthalpy of formation of solid TNDA is  $-6.7 \text{ kJ mol}^{-1}$ , which is in good agreement with the experimental data of works [4,5].

### 3.2 Combustion Mechanism

The obtained profiles indicate that the combustion rate is controlled by reactions in the condensed phase (melt), a part of the unreacted substance is ejected into the gas zone by outflowing gases, forming a narrow aerosol section above the surface, and the heat flux from the flame is spent on the evaporation of aerosol droplets, practically not reaching the surface. It would seem that this conclusion contradicts the data obtained: the thermal stability of TNDA is comparable to the stability of RDX, but the surface temperature of TNDA is much lower (Figure 6), and, therefore, the degree of TNDA decomposition in the melt will also be low and the gas-phase combustion mechanism should be realized.

To understand this contradiction, it is necessary to obtain the rate constants of the leading combustion reaction. Based on experimental data on combustion rates and surface temperatures of TNDA, the rate constants of the leading combustion reaction can be calculated. Combustion in the condensed phase is well described by the classical Zel'dovich model [32]:

$$m = \sqrt{\frac{2\rho^2\chi Q}{c_p(T_s - T_0 + L_m/c_p)^2} \left(\frac{RT_s^2}{E}\right) \cdot A \cdot e^{-E/RT_s}}$$

where  $m$ ,  $c_p$ ,  $\rho$ ,  $\chi$  are mass burning rate, specific heat, density, and thermal diffusivity of the condensed phase,  $T_s$  and  $Q$  are the surface temperature and heat of reaction,  $E$  and  $A$  are the activation energy and the preexponential factor of the leading reaction in the condensed phase. The expression  $T_s - T_0 + L_m/c_p$  accounts for warming-up of the condensed phase from initial temperature,  $T_0$ , to surface temperature,  $T_s$ , and melting. The average specific heat of the condensed phase,  $c_p$ , was taken as  $1464 \text{ J} \cdot \text{kg}^{-1} \cdot \text{K}^{-1}$ , heat of melting,  $L_m$ , was taken according to DSC data [14]. The heat of reaction  $Q$ , was taken as  $1255 \text{ J g}^{-1}$  as the heat released in the first flame.

As can be seen from Figure 7, the obtained constants ( $k_{rb} = 3.4 \cdot 10^{15} \cdot \exp(-18760/T)$ ,  $E_a = 156.1 \text{ kJ mol}^{-1}$ ) are in good agreement with the kinetics of autocatalysis obtained at lower temperatures. Thus, in contrast to the autocatalysis

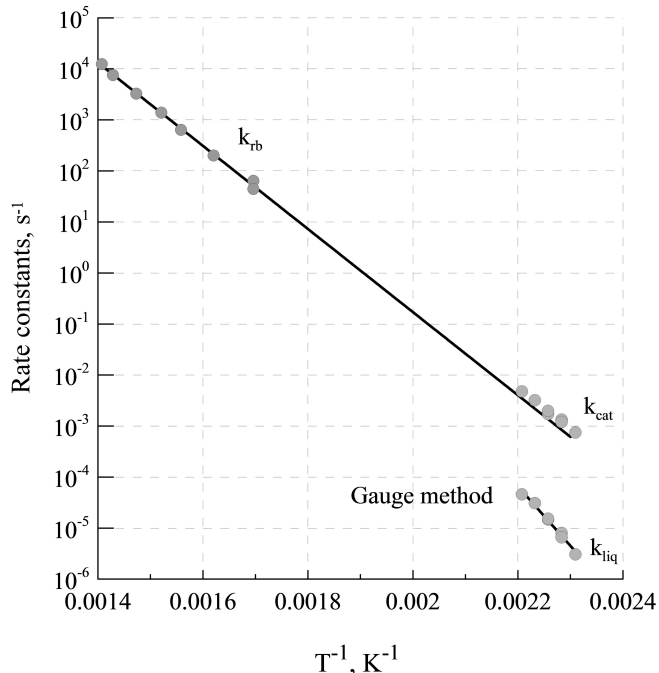


Figure 7. Kinetics of the leading combustion reaction TNDA ( $k_{rb}$ ) and decomposition under isothermal conditions ( $k_{liq}$ ,  $k_{cat}$ ).

that occurs during the decomposition of nitroesters, in the case of TNDA it is the autocatalytic reaction that becomes decisive during combustion. And this explains why, at a lower surface temperature compared to RDX, the reaction in the TNDA melt controls the burning rate.

### 4 Conclusion

The thermal decomposition of 1,3,5,5-tetranitrohexahydopyrimidine (TNDA) in liquid phase, in contrast to parent RDX, is accompanied by strong autocatalysis. The proposed mechanism of this process allows us to remove the apparent contradictions of previously obtained experimental data. The essence of autocatalysis is the oxidation of TNDA by decomposition products with the subsequent destruction of the entire molecule. An unusual feature of autocatalysis is that, unlike autocatalysis of nitroesters, this process does not disappear at high temperatures, but, on the contrary, determines the kinetics of heat release in the combustion wave. Despite the presence of strong autocatalysis, the thermal stability of TNDA is close to that of RDX.

The surface temperature and combustion mechanism of TNDA were established with the help of thermocouple studies. It turned out that the replacement of the nitramine group with a dinitromethyl fragment leads to an increase in volatility. Nevertheless, despite the lower surface temperature of TNDA as compared to RDX, the combustion mechanism of both substances is the same. This is due to the fact that, unlike RDX, the rate of heat release at the sur-

face temperature is determined not by the kinetics of the initial bond breaking, but by the fast kinetics of autocatalysis.

## Acknowledgements

The authors would like to acknowledge Dr. Ruth Doherty for help in editing and valuable remarks and discussion. This research was supported by the Ministry of Science and Higher Education of the Russian Federation (Agreement with Zelinsky Institute of Organic Chemistry RAS No 075-15-2020-803).

## Data Availability Statement

The data that support the findings of this study are openly available in this paper.

## References

- [1] D. A. Levins, C. D. Bedford, S. J. Staats, Synthesis of 1,3,5,5-tetranitrohexahydropyrimidine. *Propellants Explos. Pyrotech.* **1983**, *8*, 74–76.
- [2] D. L. Levins, C. D. Bedford, C. L. Coon, *1,3,5,5-Tetranitrohexahydropyrimidine (DNNC)*, US Patent, 4,346,222 (24 Aug. 1982), SRI International, Menlo Park, California, US.
- [3] Y. Oyumi, T. B. Brill, A. L. Rheingold, T. M. Haller, Crystal structure and molecular dynamics of the energetic nitramine 1,3,5,5-tetranitrohexahydropyrimidine and a comparison with 1,3,3,5,7,7-hexanitro-1,5-diazacyclooctane and 1,3,3-trinitroazetidine. *J. Phys. Chem.* **1985**, *89*, 4317–4324.
- [4] S. Bourasseau, A systematic procedure for estimating the standard heats of formation in the condensed state of non aromatic polynitro-compounds. *J. Energ. Mater.* **1990**, *8*, 266–291.
- [5] H.-H. Licht, H. Ritter, Neue Sprengstoffe: Ihre Leistung in Theorie und Praxis, *Proc. 21st Inter. Annual Conf. of ICT*, **1990**.
- [6] J. Boileau, M. Piteau, G. Jacob, Synthèse de la 1,3,5,5-tetranitrohexahydropyrimidine, *Propellants Explos. Pyrotech.* **1990**, *15*, 38.
- [7] G. Singh, I. P. S. Kapoor, S. M. Mannan, S. K. Tiwari, Studies on energetic compounds: Part XI: Preparation and thermolysis of polynitro organic compounds. *J. Hazard. Mater.* **1999**, *68*, 155–178.
- [8] H. S. Jadhav, M. B. Talawar, R. Sivabalan, D. D. Dhavale, S. N. Ashtana, V. N. Krishnamurthy, Synthesis, characterization and thermolysis of polynitrohexahydropyrimidines: Potential high energy materials, *Indian J. Eng. Mater. Sci.* **2006**, *13*, 80–86.
- [9] L.-J. Zhang, Y.-P. Ji, B. Chen, F. Ding, D.-P. Li, W.-X. Liu, Synthesis of 1,3,5,5-Tetranitrohexahydropyrimidine with high yield, *Chinese J. Energ. Mater.* **2012**, *20*, 441–444.
- [10] M. Li, F.-Q. Zhao, S.-Y. Xu, E.-G. Yao, Q. Pei, H.-X. Hao, H.-Y. Jiang, Effect of ammonium perchlorate replacements on energetic performance of solid propellant, *Chinese J. Explos. Propellants* **2016**, *39*, 86–91.
- [11] H. Ritter, H. H. Licht, Synthesis and Explosive Properties of 1,3,5-Trinitrohexahydropyrimidine (TNP) and 5-Nitroxymethyl-
- 1,3,5-trinitrohexahydropyrimidine (NMP), *Propellants Explos. Pyrotech.* **1985**, *10*, 147.
- [12] M. A. Hiskey, D. L. Naud, Improved synthetic routes to poly-nitroheterocycles, *J. Energ. Mater.* **1999**, *17*, 379.
- [13] D. V. Katorov, G. F. Rudakov, V. V. Parakhin, I. N. Barannikova, V. F. Zhilin, Synthesis of energetic derivatives of 1,3,5-trinitrohexahydropyrimidine, *Ammunition and Special Chem.* **2008**, 42–46 (in Russian).
- [14] S. A. Shackelford, Heat of Fusion for 1,3,5,5-Tetranitrohexahydropyrimidine (DNNC) and its DNNC-d<sub>6</sub> deuterium labelled analogue, *Propellants Explos. Pyrotech.* **1995**, *20*, 1–4.
- [15] S. A. Shackelford, J. A. Menapace, J. F. Goldman, Liquid state thermochemical decomposition of neat 1,3,5,5-tetranitrohexahydropyrimidine (DNNC) and its DNNC-d<sub>2</sub>, DNNC-d<sub>4</sub>, DNNC-d<sub>6</sub> structural isotopomers: mechanistic entrance into the DNNC molecule, *Thermochim. Acta* **2007**, *464*, 42–58.
- [16] Y. Oyumi, T. B. Brill, Thermal decomposition of energetic materials 4. High-rate, in situ, thermolysis of the four, six, and eight membered, oxygen-rich, gem-dinitroalkyl cyclic nitramines, TNAZ, DNNC, and HNDZ. *Comb. Flame* **1985**, *62*, 225–231.
- [17] T. B. Brill, D. G. Patil, J. Duterte, G. Lengelle, Thermal decomposition of energetic materials 63. Surface reaction zone chemistry of simulated burning 1,3,5,5-tetranitrohexahydropyrimidine (DNNC or TNDA) compared to RDX. *Comb. Flame* **1993**, *95*, 183–190.
- [18] Q. Zhao, S. Zhang, Q. S. Li, The influence of ring strain and conjugation on the reaction energies of the NO<sub>2</sub> fission of nitramines: A DFT study. *Chem. Phys. Letters* **2005**, *407*, 105–109.
- [19] R. S. Stepanov, L. A. Kruglyakova, A. M. Astakhov, Effect of the structure of cyclic N-nitramines on the rate and mechanism of their thermolysis, *Russ. J. Gen. Chem.* **2007**, *77*, 1211–1217.
- [20] H. E. Kissinger, Reaction kinetics in differential thermal analysis, *Analyt. Chem.* **1957**, *29*, 1702–1706.
- [21] G. B. Belov, Thermodynamic analysis of combustion products at high temperature and pressure. *Propellants Explos. Pyrotech.* **1998**, *23*, 86–89.
- [22] A. E. Fogelzang, V. Yu Egorshev, V. P. Sinditskii, M. D. Dutov, Combustion of nitroderivatives of azidobenzenes and benzofuroxans, *Comb. Flame* **1991**, *87*, 123–135.
- [23] A. I. B. Robertson, The thermal decomposition of explosives. II: Cyclotrimethylenetrinitramine and cyclotetramethylenetrinitramine, *Trans. Faraday Soc.* **1949**, *45*, 85–93.
- [24] G. B. Manelis, G. M. Nazin, Yu.I. Rubtsov, V. A. Strunin, *Thermal Decomposition and Combustion of Explosives and Propellants*. CRC Press, **2003**.
- [25] B. S. Svetlov, V. P. Shelaputina, L. B. Gorodkova, Effect of the structure of nitrate esters on the rate of their acid hydrolysis, *Kinetika i Kataliz* **1972**, *13*, 880–884 (in Russian).
- [26] P. M. Esteves, J. W. de M Carneiro, S. P. Cardoso, A. G. H. Barboza, K. K. Laali, G. Rasul, G. K. Surya Prakash, G. A. Olah, Unified mechanistic concept of electrophilic aromatic nitration: convergence of computational results and experimental data. *JACS* **2003**, *125*, 4836–4849.
- [27] E. Drent, W. P. Mul, A. A. Smaardijk, Polyketones, in *Encyclopedia of Polymer Science and Technology*, **2002**, 4<sup>th</sup> ed., Vol. 3, edited Wiley & Sons, Inc.
- [28] V. P. Sinditskii, V. Yu Egorshev, M. V. Berezin, V. V. Serushkin, S. A. Filatov, A. N. Chernyi, Combustion mechanism of nitro ester binders with nitramines, *Combust. Explos. Shock Waves* **2012**, *48*, 163–176.
- [29] V. P. Sinditskii, V. Y. Egorshev, V. V. Serushkin, A. I. Levshenkov, M. V. Berezin, S. A. Filatov, Combustion of energetic materials governed by reactions in the condensed phase. *Inter. J. Energ. Mater. Chem. Propulsion* **2010**, *9*, 147–192.

- [30] V. P. Sinditskii, V. Yu Egorshev, V. V. Serushkin, A. I. Levshenkov, M. V. Berezin, S. A. Filatov, S. P. Smirnov, Evaluation of decomposition kinetics of energetic materials in the combustion wave. *Thermochim. Acta* **2009**, *496*, 1–12.
- [31] G. Jacob, S. Benazet, R. Tryman, P. Goede, H. Oestmark, Calculations of densities and heats of formations of energetic molecules for the use in thermochemical codes, *Proc. 8th Seminar "New Trends in Research of Energetic Materials"*, Pardubice, Czech Republic, Apr. 19–21, **2005**, Vol. 1, 222–231.
- [32] Y. B. Zel'dovich, Theory of combustion of propellants and explosives. *Zh. Eksp. Teoret. Fiziki* **1942**, *12*, 498–524.

Manuscript received: October 3, 2020

Revised manuscript received: October 10, 2020

Version of record online: December 3, 2020